Magneto-optical properties of chromium-alloyed manganese bismuth thin films

Prabhakar R. Bandaru[a] and Timothy D. Sands
Department of Materials Science and Mineral Engineering, University of California, Berkeley, California 94720

Dieter Weller and Ernesto E. Marinero
IBM Research Division, Almaden Research Center, 650 Harry Road, San Jose, California 95120

(Received 22 December 1998; accepted for publication 22 April 1999)

MnBi thin films have been considered for short-wavelength rewritable optical recording media due to the very large magneto-optic Kerr rotation and perpendicular anisotropy (K_u) of the hexagonal magnetic low-temperature MnBi phase. However, coincident structural and magnetic transformations near the Curie temperature (360 °C) result in poor thermal cycling behavior, preventing the application of MnBi as rewritable media. We have previously hypothesized that the substitution of Cr for Mn would reduce the ferromagnetic coupling along the *c* axis, thereby lowering the Curie temperature and possibly decoupling the magnetic and structural transitions. Preliminary experimental data reported earlier [P. R. Bandaru *et al.*, Appl. Phys. Lett. **72**, 2337 (1998)] supported this hypothesis. In this article, the effects of Cr substitution are further explored and the feasibility of $Mn_{1-x}Cr_xBi$ ($0<x<0.15$) films for magneto-optical recording applications analyzed. It is shown that 5% Cr is sufficient for decoupling the phase transitions with no significant loss in the magneto-optic figure of merit. Transmission electron microscopy studies indicate a small grain size (~50 nm) for the Cr-alloyed films, which could be beneficial for reducing media noise.
 [S0021-8979(99)04515-6]

I. INTRODUCTION

Of the candidate media[1–3] for ultra-high-density rewritable magneto-optical recording, polycrystalline MnBi thin films are unsurpassed in two of the most important criteria, the magnitude of the Kerr signal in the blue-wavelength regime and the degree of perpendicular anisotropy (K_u). Attempts to exploit these properties have revealed poor thermal cycling behavior and high media noise, both of which are attributed in part to hysteresis in the first-order magnetic and crystallographic phase transformation at 360 °C between the low-temperature phase (LTP) and the high-temperature phase (HTP).[4] In magneto-optic recording, the high-temperature phase is quenched and the simultaneous presence of the LTP and the quenched HTP (QHTP) is a source of media noise. Furthermore, the high Curie temperature of 360 °C necessitates high laser power during writing and allows for only a small margin of error since MnBi decomposes at around 450 °C.[5] An additional source of concern in the polycrystalline films is the large grain size, which causes large readout noise because the written domains tend to follow the grain boundaries.[6]

Several attempts have been made to eliminate each of these problems. The attempts at stabilizing one of the phases (LTP or the QHTP) mainly focused on retarding the kinetics of the transformation by substituting one or more elements [Cu, Sc, V, Cr, Fe, Co, Ni, Zn, Ti;[7] Ru, Rh;[8] Cu;[9] Al (Refs. 10–12)] into the MnBi crystal structure to form stable compounds. Although sufficient stabilization was achieved in some cases[7–9] there was usually a significant loss in the figure of merit (defined by the product of reflectivity: *R* and remanent Kerr rotation: θ_k, as $R^{1/2}\theta_k$) and the formation of extraneous phases.[7,9]

Bearing in mind the earlier attempts to solve the phase stability problem, it is apparent that the coincident structural and magnetic phase transition at 360 °C remains the principal impediment to the effective demonstration of MnBi as a magneto-optic recording medium. The research reported here was initiated with the primary objective of decoupling the magnetic transition from the first-order structural transition. Furthermore, melting of Bi inclusions at temperatures above the MnBi–Bi eutectic at 265 °C has been observed to have a catastrophic effect on the microstructural integrity of MnBi.[13] Hence, a magnetic transition below 265 °C would be desirable. In a previous publication,[14] we had argued that Cr substituted for Mn should have the desired effect of reducing the transition temperature.

Before elaborating on this hypothesis and the associated experimental data, it is necessary to review the structure and magnetic properties of MnBi.

A. Structure and magnetic properties of MnBi

The equilibrium low-temperature phase of MnBi adopts the hexagonal NiAs ($P6_3/mmc$) structure (Fig. 1) with $a_0 = 0.4290$ nm and $c_0 = 0.6126$ nm at room temperature. The Mn^{3+} ions are in the octahedral interstices of the hexagonal close-packed Bi sublattice and form a simple hexagonal sublattice. Along the *c* axis the octahedral sites share common faces both above and below, and the cations are arranged in linear chains. The tetrahedral interstices of the anion sublat-

[a]Electronic mail: Prabhakar_Bandaru@amat.com

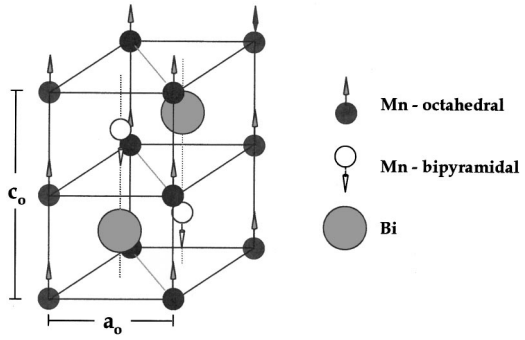

FIG. 1. Crystal structure of the MnBi low-temperature phase (LTP). The Bi anions form a hexagonal close-packed sublattice. The Mn ions are situated in the octahedral interstices and partially occupy the bipyramidal interstices leading to a (c/a) ratio of ~1.4. The arrows on the Mn ions correspond to a hypothesized ferromagnetic unit.

tice also share a common face, and each tetrahedral site pair forms a single trigonal bipyramidal hole, which is thus five-fold coordinated. These bipyramidal interstices are sufficiently large to accommodate additional cations (for an ideal hexagonal close-packed lattice, the c/a ratio is 1.633; however, in MnBi the ratio is ~1.4, indicative of the presence of interstitials).

During heating through 360 °C in the magneto-optical recording process (Fig. 2), a coupled magnetic and first-order lattice transition results in the formation of a paramagnetic or antiferromagnetic[15,17] high-temperature phase. This transformation is believed[16,17] to involve the shuffle of 15% of the Mn from the octahedral lattice sites to the bipyramidal sites. Upon quenching from above 360 °C, the HTP can be retained. The quenched HTP, however, is inherently unstable[4] and transforms back to the low-temperature phase over a period of two years. In magneto-optic recording, the simultaneous presence of the LTP and the quenched HTP contributes to media noise.

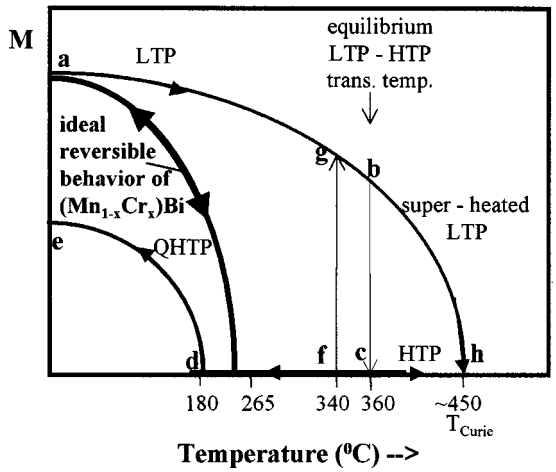

FIG. 2. Cr addition to MnBi ideally results in a reversible phase transformation avoiding the phase inhomogeneity problem inherent to MnBi. The transformation temperature is also reduced to below the MnBi–Bi eutectic temperature of ~265 °C due to the decoupling of the structural and magnetic phase transformations. A typical recording cycle on the MnBi system $(a \rightarrow b \rightarrow c \rightarrow d \rightarrow e)$ by Curie point writing is shown. On heating $(a \rightarrow b)$, the low-temperature phase (LTP) of MnBi undergoes an irreversible first-order phase transformation $(b \rightarrow c)$ to the high-temperature phase (HTP) at 360 °C. The QHTP is formed on quenching $(c \rightarrow d \rightarrow e)$ the HTP from above 360 °C. The QHTP is inherently unstable and gradually transforms back $(e \rightarrow a)$ to the LTP. In the case of slow or moderate heating, there is a temperature hysteresis $(c-f \sim 20\,°C)$ associated with this transformation, the HTP transforming back $(c \rightarrow f \rightarrow g \rightarrow a)$ only at ~340 °C. A purely magnetic phase transformation $(a \rightarrow b \rightarrow h)$ following the Brillouin law gives a ''true'' Curie temperature of ~450 °C.

The magnetism in these phases is a source of controversy, since neutron diffraction has not been able to provide conclusive evidence.[16,17] A large part of the difficulty arises from the fact that it is extremely difficult to prepare the MnBi compound in its pure form due to a peritectic formation mechanism,[5] which invariably results in unreacted Bi and Mn. Neutron diffraction measurements[16,17] indicate a magnetic moment of $3.95\mu_B$ for the low-temperature phase and $1.90\mu_B$ for the quenched high-temperature phase. One of the authors has proposed a model[13] in the localized moment framework, where by a simple modification of the original mechanism of superexchange[18] and incorporation of crystal-field theory, one can arrive at a magnetic moment of $4\mu_B$ for the LTP and $2\mu_B$ for the quenched HTP. The differences from the experimental values may be rationalized as due to deviations from the localized moment picture. However, it is generally accepted that ferromagnetic interactions predominate, possibly mediated[19] by an exchange inversion superexchange mechanism through the Bi $6p$ orbitals.

B. Role of chromium in decoupling the magnetic and structural transitions

Chromium has a very strong preference for the octahedral site;[20] it has the highest octahedral field stabilization energy of the transition-metal ions.[21] It was also seen, in retrospect from the binary phase diagram,[22] that Cr and Bi are immiscible and do not form compounds; this would eliminate some of the earlier problems associated with the formation of extraneous phases.[7–9] It was noticed at the time of writing this article, that the alloying of Cr with MnBi was attempted before[7] without success. Nevertheless, it is clear for the aforementioned reasons that Cr substitution is a promising approach, as the present study has confirmed.

It was seen in this research that the substitution of Cr (up to $x=0.15$ in $Mn_{1-x}Cr_xBi$) has the desired effect of reducing the transformation temperature to ~250 °C. In this article, the microstructural and magnetic properties of Cr-alloyed MnBi films are presented in detail.

II. EXPERIMENT

Electron-beam deposition (10^{-6} Torr base pressure), was used to sequentially deposit Bi, Mr, and Cr on silica glass disk substrates (Hoya Industries) and silicon nitride (60 nm/silicon substrates Fig. 3). The former substrates are equivalent to that likely to be used in magneto-optical recording application, whereas the latter permit straightforward fabrication of plan-view transmission electron microscopy (TEM) samples. The substrates were ultrasonically cleaned, successively in soapy water, acetone, isopropanol, and deionized water. At each stage dry nitrogen was used for

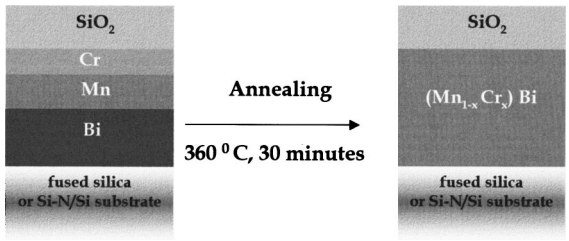

FIG. 3. Schematic of the $Mn_{1-x}Cr_xBi$ thin-film preparation process, illustrating the optimal annealing conditions. The SiO_2 capping layer is used to protect the films from the ambient.

drying the substrates before immersion in the next cleaning agent. It was found that the quality of the films depends very critically on the cleanliness of the substrates.

The deposition of Bi first is essential to the development of good *c*-axis texture in MnBi-based thin films. The Bi is highly textured as deposited and this texture is imparted to MnBi as it nucleates at the Mn/Bi interface during heating, as was observed[13] in *in situ* transmission electron microscopy studies. It was found that a slow deposition rate of less than 2 nm/min was necessary to obtain reproducible films. The thin films were coated with 60 nm of SiO_2 for protection from the ambient.

Layer thicknesses were adjusted to yield an average composition of $Mn_{1-x}Cr_xBi$ ($0<x<0.15$) on annealing (Fig. 3). The annealing was done in vacuum (10^{-7} Torr) in the temperature range of 250–400 °C and for durations from 15 min to 2 h. X-ray diffraction (Siemens D5000) was used to determine the crystal structure and orientation. An *in situ* standard (the Si 004$K\beta$ peak) was used for the *c*-lattice parameter estimation.

Transmission electron microscopy (TEM: JEOL 200 CX) together with energy dispersive spectroscopy (EDS) was used for the examination of microstructure and for compositional determination. The films deposited on the silicon nitride/silicon substrates are amenable to TEM observations through the electron transparent silicon nitride membranes, when the silicon substrate is etched away. Auger electron spectroscopy (AES) using a Perkin–Elmer (Phi 660) scanning Auger microscope was used in the sputter profiling mode on thin films deposited on silicon substrates (quartz substrates are unsuitable due to severe charging effects) for compositional information.

The magnetic measurements were obtained through magneto-optic Kerr spectroscopy and vibrating sample magnetometry (TOEI). The Kerr hysteresis loop measurements on the thin films were obtained with a *p*-polarized He–Ne (λ: 633 nm) laser of 1.5 mm diam on the sample placed within the pole pieces of a 20 kOe magnet. The hysteresis curves were recorded perpendicular to the plane of the film, by probing the $Mn_{1-x}Cr_xBi$ films through the substrate side for the most consistent readings (±5%). Measurements taken through the front (SiO_2) capping layer exhibit greater variation of θ_k (±10%) and H_c (±25%). This variation could be due to interference effects along with variations in the capping layer thickness. Kerr measurements were performed as a function of temperature, and the Kerr rotation was assumed

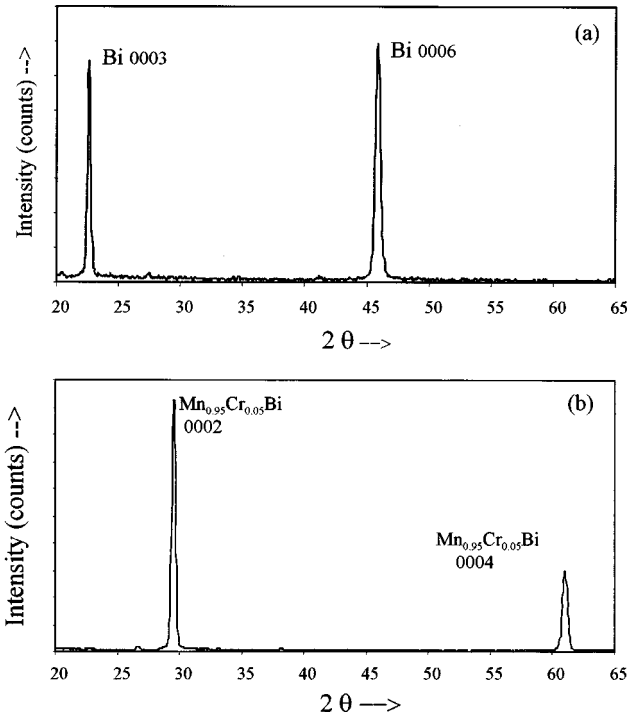

FIG. 4. (a) X-ray diffraction pattern (coupled θ–2θ scan) of an as-prepared film of $Mn_{0.95}Cr_{0.05}Bi$ on a fused silica glass substrate (108 nm, 80 nm SiO_2 cap). The patterns were similar for all the $Mn_{1-x}Cr_xBi$ films in the range $0<x<0.15$. (b) X-ray diffraction pattern (coupled θ–2θ scan) of an annealed film of $Mn_{0.95}Cr_{0.05}Bi$ on a fused silica glass substrate (108 nm, 80 nm SiO_2 cap). The patterns were similar for all the $Mn_{1-x}Cr_xBi$ films in the range $0<x<0.15$. The small peak at ~27° corresponds to $K\beta$ (λ:1.3922 Å) 0002 reflection.

to be proportional to the magnetization.[23] The temperature at which the Kerr rotation extrapolated to zero was taken as the transformation/Curie temperature. The temperature was varied in 15 °C intervals with heating and cooling rates around 40 °C/h. The films were tested for magnetic reversibility by alternate heating and cooling cycles. At least three measurements were taken at each temperature to ensure accuracy and stability.

Spectral measurements[24] of the Kerr rotation, ellipticity, and reflectance were taken through the back of the quartz substrates in air at room temperature in the range 0.8–5.5 eV (1550–225 nm). As the remanence ratio was close to 1.0, the measurements were taken in the absence of a magnetic field.

III. RESULTS AND DISCUSSION

A. X-ray diffraction

The as-prepared films of $Mn_{1-x}Cr_xBi$ showed Bi peaks in the 000l orientation [Fig. 4(a)]. As the peaks from Cr and Mn were not observed, it is plausible that they are in a fine-grained untextured polycrystalline form. The as-deposited SiO_2 is likely to be amorphous in nature. The best texture, as defined in terms of the smallest full width at half maximum (FWHM) of the rocking curves for the thin films, was obtained on annealing at 360 °C for 30 min.[14] The FWHM decreases from 3° in the as-prepared films to 1° in the annealed films, indicating refinement of the texture on annealing. The x-ray diffraction pattern for the annealed

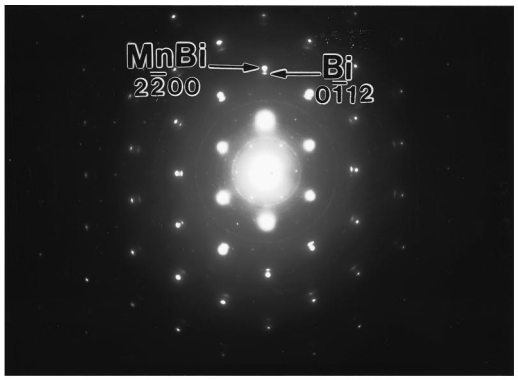

(a)

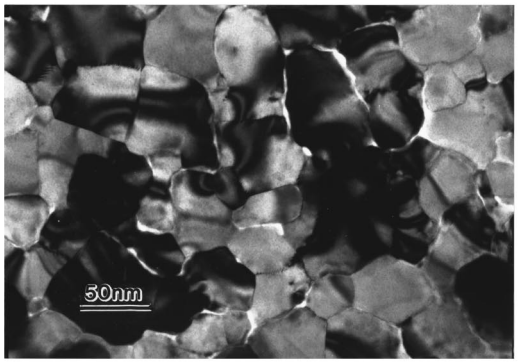

(b)

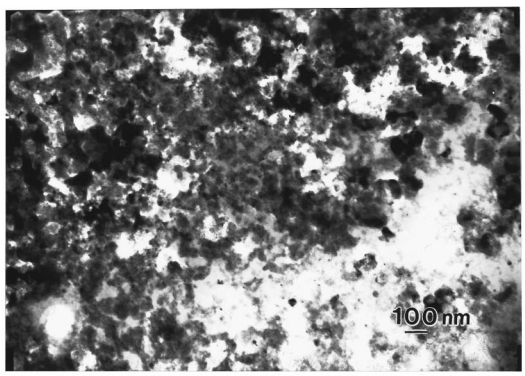

(c)

FIG. 5. (a) Selected area diffraction pattern of annealed MnBi. The pattern shows a characteristic topotaxial relationship where the underlying Bi serves as the template for MnBi growth. (b) Plan-view bright-field micrograph of an annealed MnBi film. The average grain size is about 70 nm. (c) Plan-view bright-field micrograph of annealed $Mn_{0.95}Cr_{0.05}Bi$. The grain size is in the range of 5–50 nm.

$Mn_{0.95}Cr_{0.05}Bi$ [Fig. 4(b)] is typical of the $Mn_{1-x}Cr_xBi$ ($0<x<0.15$) family. No reflections other than 000l were seen in the annealed films, indicating a high degree of *c*-axis orientation.

B. Transmission electron microscopy (TEM)

The TEM analyses of MnBi-based films establish a topotaxial relationship between the underlying Bi and MnBi [Fig. 5(a)]. The grain size in unalloyed MnBi films was of the order of 70 nm [Fig. 5(b)]. The composition inside the grains was analyzed by EDS (standardless Cliff–Lorimer[25] analysis) and confirmed to be $Mn_{50}Bi_{50}$ with a precision of

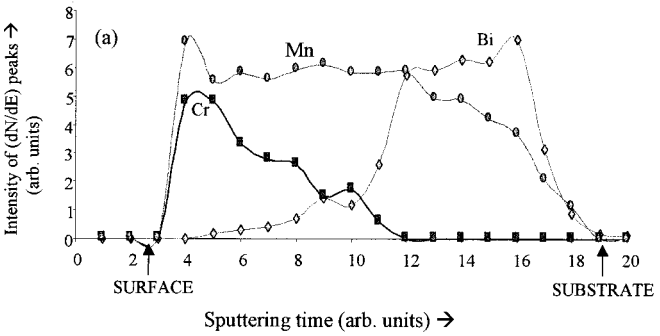

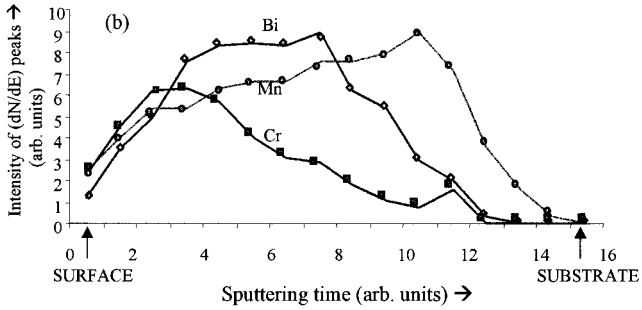

FIG. 6. (a) Auger (AES) depth profiling spectra for an as-prepared $Mn_{0.90}Cr_{0.10}Bi$ film. The different sputtering times correspond to different depths into the film and are a qualitative measure. The profiles indicate either considerable interface roughness or diffusion of the Mn into the Bi. (b) AES depth profiling spectra for an annealed $Mn_{0.90}Cr_{0.10}Bi$ film. The broadening of the Cr distribution in the annealed sample could imply diffusion of Cr into the film, however, residual Cr is present at the surface.

$\pm 2\%$. However, the films were not very uniform, and residual Bi islands and Mn inclusions were observed. EDS analyses also suggest the presence of Bi along the grain boundaries.

The microstructures in Cr-alloyed MnBi films reveal the presence of very small grains [Fig. 5(c)] in the range of 5–50 nm. Selected area diffraction studies mirror the small particle sizes, and a topotaxial relationship between Bi and $Mn_{1-x}Cr_xBi$ was evident. A deviation from the desired stoichiometry was detected in the matrix grains, and this could be due to the nonuniform dispersion of Cr. Bi islands and Mn inclusions were also seen in the $Mn_{1-x}Cr_xBi$ microstructures.

C. Auger electron spectroscopy (AES)

Auger electron spectroscopy was used to depth profile the $Mn_{1-x}Cr_xBi$ films to investigate possible surface chromium segregation, as EDS analyses note that the matrix contained less Cr than intended. Sequential sputter profiling was performed on the as-prepared and annealed $Mn_{0.90}Cr_{0.10}Bi$ films on a silicon substrate. The spectra [Figs. 6(a) and 6(b)] have a nontrivial interpretation due to the texture of the thin films and the widely different sputtering rates[26] of Bi, Mn, and Cr. However, it is seen that the distribution of elements in the annealed film is not uniform.

In the as-prepared film [Fig. 6(a)], the profile of Mn could be explained as due to either considerable diffusion of Mn into the Bi or indicative of interface roughness. Bi diffusion is seen in the annealed film [Fig. 6(b)], indicating a

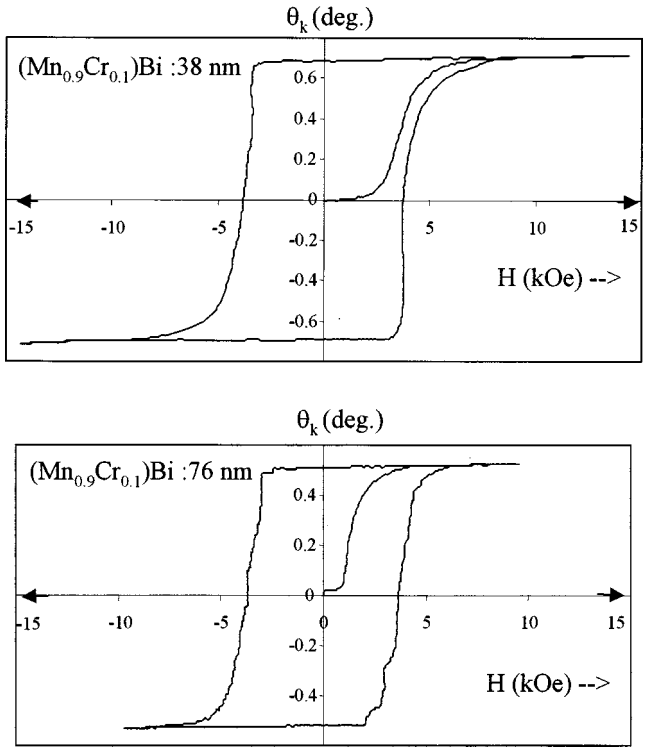

FIG. 7. Hysteresis loops for thin (38 nm) and thick (76 nm) films of $Mn_{0.90}Cr_{0.10}Bi$. The pinning mechanism is dominant in thin films whereas the nucleation mechanism of domain-wall motion dominates in thicker films. This phenomenon was found in all the MnBi and $Mn_{1-x}Cr_xBi$ films.

mixing of the Mn and Bi. Chromium, which is seen as a distinct layer in the as-prepared state, diffuses into the bulk on annealing. This conjecture is based on the broadening seen in the elemental distribution. However, there still seems to be considerable Cr at the film surface.

D. Kerr spectroscopy

Magnetic and magneto-optic properties of the $(Mn_{1-x}Cr_x)Bi$ $(0<x<0.15)$ films were investigated as a function of film thickness, composition, and temperature.

1. Film thickness

Thin films of $Mn_{1-x}Cr_xBi$ in the thickness range 20–105 nm, when saturated in the magnetic field, exhibit a remanence ratio $(=M_R/M_S)$ of ~ 1. This type of behavior is optimal for magneto-optical recording. The precise form of the hysteresis curve depends on the magnitude of the field necessary to nucleate domain walls, the critical field (H_{cr}) *vis-à-vis* the wall coercive field (H_w) necessary to nucleate domain-wall motion.[27] By comparing the virgin magnetization curve with the saturation hysteresis loop, one can distinguish between *nucleation-type* behavior, where the virgin curve is steep and saturation is reached at fields lower than the coercive field, and *pinning-type* behavior where fields of the order of the coercive field are required.[28]

In general, it was found that in thinner films the pinning mechanism is dominant, whereas the nucleation mechanism for domain-wall motion dominates in thicker films [Figs. 7(a) and 7(b)].

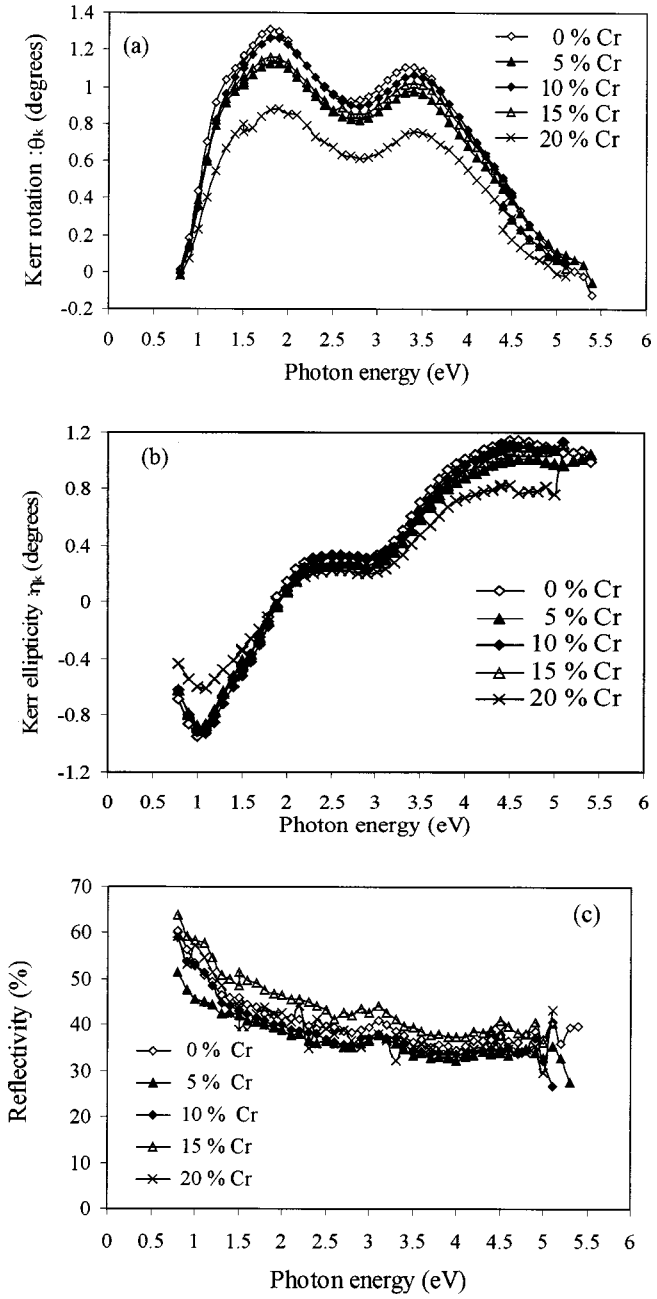

FIG. 8. Magneto-optic Kerr-effect spectra as a function of at. % Cr for $Mn_{1-x}Cr_xBi$ films: (a) rotation, (b) ellipticity, and (c) reflectance.

2. Composition: $Mn_{1-x}Cr_xBi$ $(0<x<0.15)$

Polar magneto-optic Kerr effect (MOKE) spectra were measured for single-phase MnBi and $Mn_{1-x}Cr_xBi$ films of predominant *c*-axis texture as a function of composition [Figs. 8(a) and 8(b)]. No marked dependence of the spectral Kerr effect on film thickness was observed. The spectra have not been corrected for the optical constants of the substrate.[29] The normal incidence reflectivity decreases monotonically [Fig. 8(c)] from about 60% at 0.8 eV to 35% at 5.3 eV, which precludes enhancements due to multiple reflection and interference effects.

The rotation spectra [Fig. 8(a)] display the characteristic dual-peak structure common to many ferromagnetic transition metals.[24] The peaks in the Kerr rotation occur at 1.84 eV

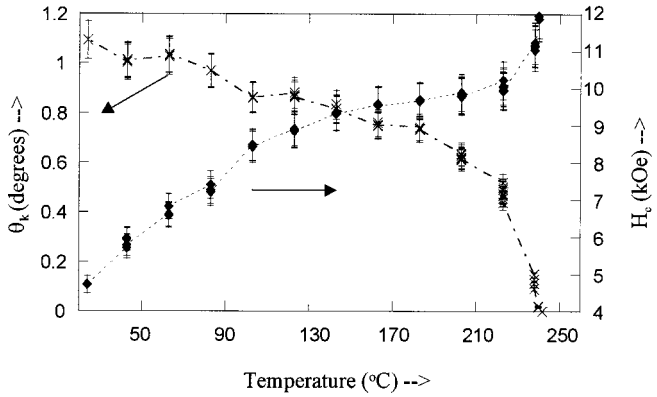

FIG. 9. Remanent Kerr rotation (θ_k) and coercivity (H_c) as a function of temperature for $Mn_{0.85}Cr_{0.15}Bi$ (108 nm thick, 80 nm SiO_2 cap) films on silicon nitride/silicon substrates.

(670 nm) and at 3.43 eV (370 nm). Regardless of its origin,[30–32] the short-wavelength peak is a technologically important attribute in that it is well matched to the band-edge emission (λ:360–450 nm) from GaN-based diode lasers.[33]

The ellipticity spectra [Fig. 8(b)] show the expected Kramers–Krönig invariant behavior[34] with a zero crossing at around the infrared Kerr rotation peak.

It is seen from Fig. 8 that the Kerr effect is not significantly diminished for chromium additions up to 15%. On comparing the spectra of the unalloyed MnBi and Cr-alloyed MnBi films, one does not observe any difference in the general shape. This suggests that Cr may not influence the states involved in the magneto-optic transitions.[35]

3. Temperature

The transformation temperature (defined here as the temperature at which the remanent Kerr rotation extrapolates to zero) of the MnBi and Cr-alloyed MnBi films as a function of thickness and composition ($0<x<0.15$), was estimated by temperature-dependent Kerr hysteresis loop measurements using a He–Ne laser (λ:633 nm).

The reduction of the remanent Kerr rotation with increased temperature (Fig. 9) is thought to be due to the turning of the magnetic moments away from the uniaxial (*c*-axis) direction. It was seen that the Cr-alloyed MnBi films exhibit much better temperature cycling and reversibility characteristics compared to the MnBi films.

It was also found that the coercive field (H_c) rapidly increases with temperature[13,14,36] and an exchange anisotropy is induced in the films (Fig. 10), as defined by a shift in the hysteresis loop to the left. The presence of exchange anisotropy,[37] characterized in terms of an exchange field (H_E, the net shift), may represent a new phenomenon associated with the MnBi system. A plausible reason involves the fluctuation in Mn concentration that leads to a coexistence of magnetic interactions. This fluctuation could be brought about by the shift of the Mn atoms from the octahedral lattice sites to the bipyramidal interstitial sites[16,17] with increasing

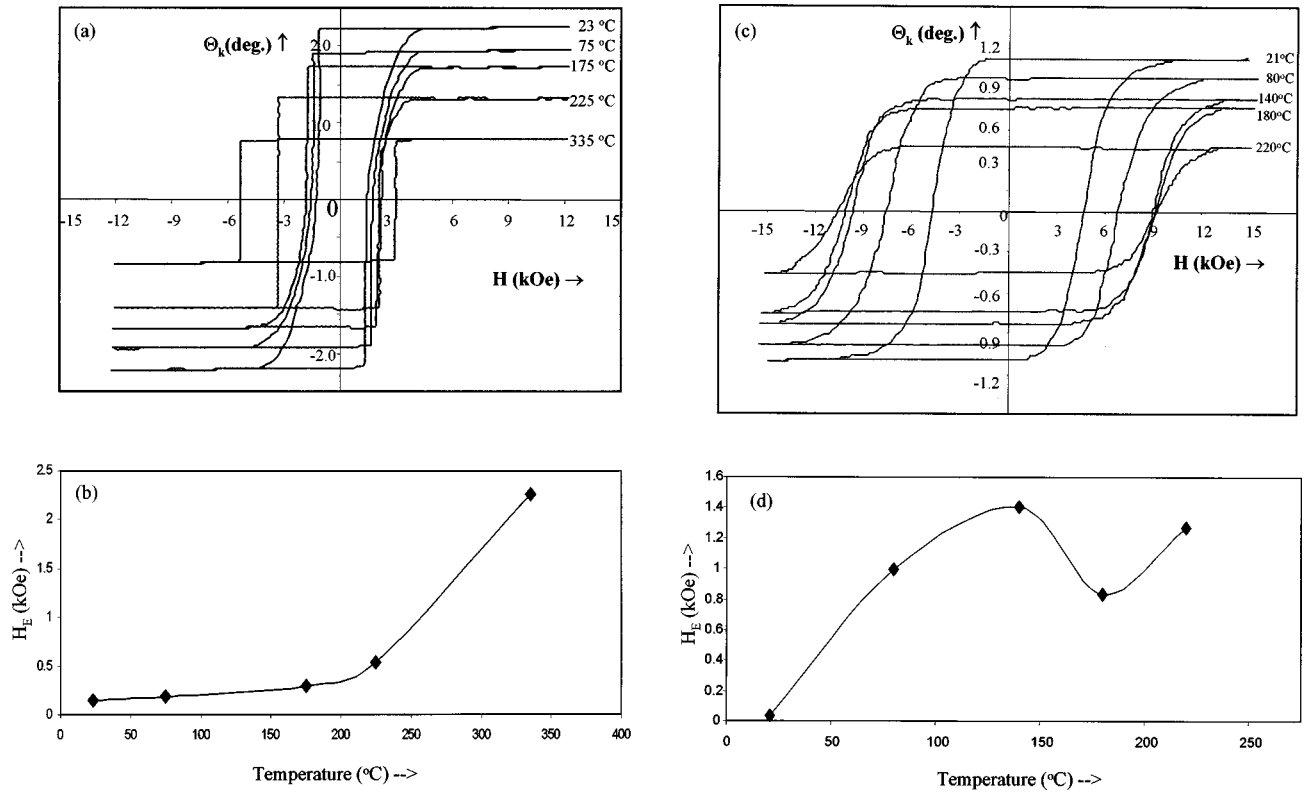

FIG. 10. (a) Hysteresis loops show an exchange anisotropy in MnBi films (108 nm, 80 nm SiO_2 cap) as the temperature is increased. (b) Variation of the exchange field (H_E) with temperature for MnBi, as measured by a net shift in the loop. (c) Hysteresis loops show an exchange anisotropy in $Mn_{0.85}Cr_{0.15}Bi$ films (108 nm, 80 nm SiO_2 cap) as the temperature is increased. (d) Variation of the exchange field (H_E) with temperature in $Mn_{0.85}Cr_{0.15}Bi$.

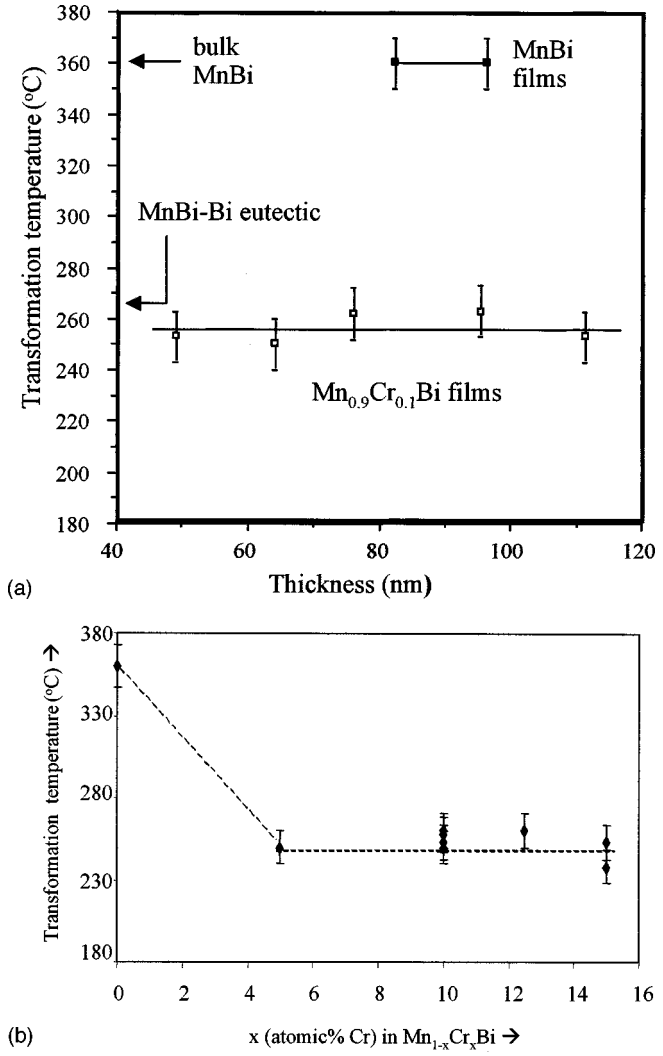

FIG. 11. (a) Variation of the transformation/Curie temperature (at which the remanent Kerr rotation extrapolates to zero) with film thickness for $Mn_{0.90}Cr_{0.10}Bi$. The capping layer of SiO_2 was 80 nm thick. (b) Variation of the transformation temperature with at. % Cr (x) up to 15%, in $Mn_{1-x}Cr_xBi$.

temperature. The presence of competing ferro- and ferrimagnetic interactions would then result in exchange anisotropy.[37] As long as the temperature is below a magnetic disordering temperature (T_{Curie} or $T_{\text{Néel}}$) this explanation may be valid.

There is a steady increase of H_E in MnBi films [Fig. 10(b)], whereas H_E in Cr-alloyed MnBi films [Fig. 10(d)] exhibits a minimum at ~180 °C. This coincides with the temperature at which the exchange coupling effects in MnBi become appreciable, an observation that is currently not understood.

The constancy of the transformation/Curie temperature for the $Mn_{1-x}Cr_xBi$ ($0<x<0.15$) as a function of thickness [Fig. 11(a)] suggests that this is an intrinsic property of this material. The transformation/Curie temperature dependence as a function of composition [Fig. 11(b)] indicates that 5% Cr suffices to reduce the transformation temperature to ~250 °C. This observation is consistent with Auger spectroscopy analyses (Fig. 6), where surface segregation of Cr was observed in the $Mn_{0.90}Cr_{0.10}Bi$ film.

IV. CONCLUSIONS

In summary, it was seen that the partial substitution of Cr for Mn in MnBi film reduces the LTP–HTP transformation temperature from 360 to 250 °C (this reduction of the transformation temperature was also theoretically confirmed in research initiated by the author[38]), without significant penalty in the magneto-optic properties. In this way, the decoupling of the magnetic and the structural transformation has been accomplished. The Bi–MnBi eutectic transformation temperature is also bypassed.

The fact that there is no penalty in the figure of merit together with the fact that there are no extraneous phases observed, is seen as one of the chief merits of alloying MnBi films with Cr. Anecdotal evidence shows that the Cr-alloyed MnBi films retain their metallic luster while the MnBi thin films are prone to corrosion, suggesting the beneficial effect of Cr. $Mn_{1-x}Cr_xBi$ films are thus more stable, due to their endurance under temperature cycling and greater corrosion resistance. In addition, microstructural analyses reveal small grain sizes in the Cr-alloyed films, which is seen as a potential advantage for recording applications.

While some progress in understanding the issues involved in the MnBi phase transformation has been made in this research, many issues remain to be resolved and understood. The principal one is the true nature of the temperature at which the Kerr rotation extrapolates to zero.[23] A ferromagnetic–antiferromagnetic transition cannot be ruled out as a possible explanation.[16,17] A study of this issue could yield some insight as to why the coercivity increases, from a more fundamental point of view. The lack of homogeneity in MnBi-based films, caused in part by the peritectic formation mechanism, has long been a difficult problem to get past. A low-temperature synthesis technique, preferably with a maximum temperature below 265 °C, may be required. While $Mn_{1-x}Cr_xBi$ is not yet ready for practical magneto-optical recording application, continued research in this area would help in understanding the magnetic interactions in Mn-based compounds which seem to be promising magneto-optical systems.[23] The potential of these films for perpendicular magnetic recording is another avenue of research.

ACKNOWLEDGMENTS

This work was supported by NSF Grant No. ECS-9409730. The use of the facilities of the Berkeley Microfabrication Laboratory, Integrated Materials Laboratory (NSF Grant DMR-9214370) and the Lawrence Berkeley National Laboratory are acknowledged. The magnetic measurements were performed at the IBM Almaden Research Center, San Jose. The assistance provided by Yukiko Kubota was invaluable throughout this project.

[1] D. Chen, G. N. Otto, and F. M. Schmit, IEEE Trans. Magn. **MAG-9**, 66 (1973).
[2] E. Sawatzky and G. B. Street, J. Appl. Phys. **44**, 1789 (1973).
[3] P. Chaudhari, J. J. Cuomo, and R. J. Gambino, Appl. Phys. Lett. **22**, 337 (1973).
[4] D. Chen, J. F. Ready, and E. Bernal, J. Appl. Phys. **39**, 3916 (1968).
[5] H. Okamoto, in *Binary Alloy Phase Diagrams*, edited by H. Okamoto and P. R. Subramanian (ASM International, Materials Park, OH, 1990).
[6] W. K. Unger and H. Harms, Appl. Phys. **2**, 191 (1973).

[7] H. Göbel, E. Wolfgang, and H. Harms, Phys. Status Solidi A **34**, 553 (1976); **35**, 89 (1976).
[8] K. Lee, J. C. Suits, and G. B. Street, Appl. Phys. Lett. **26**, 27 (1975).
[9] A. Katsui, J. Appl. Phys. **47**, 3609 (1976).
[10] G. Q. Di, Ph.D. thesis, Nagoya (unpublished).
[11] D. J. Sellmyer, R. D. Kirby, J. Chen, K. W. Wierman, J. X. Shen, Y. Liu, B. W. Robertson, and S. S. Jaswal, J. Phys. Chem. Solids **56**, 1549 (1995).
[12] Y. J. Wang, J. Magn. Magn. Mater. **84**, 39 (1990).
[13] P. R. Bandaru, Ph.D. thesis, University of California at Berkeley, 1998 (unpublished).
[14] P. R. Bandaru, T. D. Sands, Y. Kubota, and E. E. Marinero, Appl. Phys. Lett. **72**, 2337 (1998).
[15] R. R. Heikes, Phys. Rev. **99**, 446 (1955).
[16] B. W. Roberts, Phys. Rev. **104**, 607 (1956).
[17] A. F. Andresen, W. Halg, P. Fischer, and E. Stoll, Acta Chem. Scand. **21**, 1543 (1967).
[18] P. W. Anderson, Phys. Rev. **115**, 2 (1959).
[19] J. B. Goodenough, A. Wold, R. J. Arnott, and N. Menyuk, Phys. Rev. **124**, 373 (1961).
[20] J. B. Goodenough, *Magnetism and the Chemical Bond* (Wiley, New York, 1967).
[21] A. West, *Solid State Chemistry and Its Applications* (Wiley, New York, 1984).
[22] M. Venkataraman and J. P. Neumann, in *Binary Alloy Phase Diagrams*, edited by H. Okamoto and P. R. Subramanian (ASM International, Materials Park, OH, 1988).
[23] The assumption that the Kerr rotation is proportional to the net magnetization is contentious [K. H. J. Buschow, P. G. van Engen, and R. Jongebreur, J. Magn. Magn. Mater. **38**, 1 (1983)]. It remains to be demonstrated that the net magnetization is zero at the same temperature that θ_k extrapolates to zero.
[24] D. Weller, *Spin-Orbit Influenced Spectroscopies of Magnetic Solids* (Springer, Berlin, 1996), pp. 1–28.
[25] D. B. Williams and C. B. Carter, *Transmission Electron Microscopy* (Plenum, New York, 1996).
[26] L. E. Davis, N. C. MacDonald, P. W. Palmberg, G. E. Riach, and R. E. Weber, *Handbook of Auger Electron Spectroscopy* (Perkin–Elmer, Eden Prairie, MN, 1978).
[27] R. S. Tebble and D. J. Craik, *Magnetic Materials* (Wiley-Interscience, New York, 1969).
[28] G. Bertotti, *Hysteresis in Magnetism* (Academic, New York, 1998).
[29] *Handbook of Optical Constants of Solids II*, edited by E. D. Palik (Academic, Boston, MA, 1991).
[30] R. F. Sabiryanov and S. S. Jaswal, Phys. Rev. B **53**, 313 (1996).
[31] J. Köhler and J. Kübler, Physica B **237-238**, 402 (1996).
[32] H. Fu, Z. Yan, S. K. Lee, and M. Mansuripur, J. Appl. Phys. **78**, 4076 (1995).
[33] S. J. Pearton and C. Kuo, MRS Bull. **22**, 17 (1997).
[34] R. M. White, *Quantum Theory of Magnetism*, 2nd ed. (Springer, New York, 1983).
[35] R. Coehoorn and R. A. de Groot, J. Phys. F **15**, 2136 (1985).
[36] X. Guo, X. Chen, Z. Altounian, and J. O. Ström-Olsen, J. Appl. Phys. **73**, 6275 (1993).
[37] W. H. Meiklejohn, J. Appl. Phys. **33**, 1328 (1962).
[38] R. F. Sabiryanov and S. S. Jaswal (unpublished).